Reduced rank MIMO-OFDM channel estimation for high speed railway communication using 4D GDPS sequences

Farnoosh Talaei, Xiaodai Dong

December 2017

KICS The Korean Institute of Communications and Information Sciences

Available online at www.sciencedirect.com

ScienceDirect

ICT Express 3 (2017) 164–170

www.elsevier.com/locate/icte

Reduced rank MIMO-OFDM channel estimation for high speed railway communication using 4D GDPS sequences☆

Farnoosh Talaei*, Xiaodai Dong[1]

University of Victoria, Victoria, BC, V8P 5C2, Canada

Received 14 September 2017; accepted 15 November 2017
Available online 12 December 2017

Abstract

This paper presents a reduced rank channel estimator for multiple-input multiple-output orthogonal frequency-division multiplexing (MIMO-OFDM) high speed railway (HSR) systems. Conventional interpolation based channel estimators require high pilot load for robust estimation of the rapidly time varying frequency-selective MIMO-OFDM HSR channel. To relax the high pilot overhead requirement, we take advantage of the channel's restriction to low dimensional subspaces due to the time, frequency and spatial correlation and propose a low complexity linear minimum mean square error (LMMSE) channel estimator. The channel estimator utilizes a four-dimensional (4D) basis expansion channel model obtained from band-limited generalized discrete prolate spheroidal (GDPS) sequences. Simulation results validate that the mean square estimation error of the proposed estimator is smaller than that of the conventional interpolation based least square (LS) estimator and the performance is robust to different delay, Doppler and angular spreads.

Keywords: Time variant channel estimation; High speed trains; GDPS sequences; MIMO-OFDM

1. Introduction

With the fast development of high speed railways (HSRs), wireless communication for high speed trains has attracted growing attentions in recent years. Wireless communication for HSRs has many important applications, including train safety, broadband communication services for passengers such as internet access and high quality voice or mobile video broadcasting [1]. A main challenge of wireless communication for HSR is the rapidly time-varying and non-stationary propagation channel which together with the presence of line-of-sight (LOS) component and limited number of scatterers in most of the HSR scenarios, leading to violation of the wide sense stationary uncorrelated scattering (WSSUS) condition [1]. Thus robust channel estimation and equalization are required for reliable HSR wireless communication.

Pilot aided orthogonal frequency-division multiplexing (OFDM) channel estimation approaches can be divided into three groups, namely, interpolation based schemes, parametric model (PM) approaches and basis expansion models. The conventional interpolation based schemes use multi-dimensional interpolation of the estimated channel frequency response at pilots for reconstructing the channel at data locations. Papers [2] and [3] use 2D and 3D interpolation for single-input single-output (SISO) and multiple-input multiple-output (MIMO) OFDM channel estimation, respectively. The PM channel estimation schemes, use pilot symbols for directly estimating the multipath channel parameters such as the number of paths, path gains and delays, angles of arrival (AOAs) and angles of departure (AODs). The PM channel estimators have improved performance compared to the interpolation based schemes for the sparse multipath channels which can be modelled using a few number of parameters [4].

However, for rapidly time variant frequency selective channels both the interpolation based and PM schemes require

* Corresponding author.
E-mail address: ftalaei@uvic.ca (F. Talaei).
[1] Senior Member, IEEE.
Peer review under responsibility of The Korean Institute of Communications Information Sciences.
☆ This paper is part of a special section titled "Special Issue on Intelligent Transportation Communication Systems" guest edited by Prof. Zonghua Gu, Prof. Shigang Yue, Prof. Sanghyun Ahn, Prof. Juan-Carlos Cano, Prof. Joel Rodrigues, Prof. Houbing Song, Prof. Hai L. Vu, Prof. Danda Rawat, Prof. Dongkyun Kim.

https://doi.org/10.1016/j.icte.2017.11.005

high pilot overhead for tracking the time variation of the channel coefficients or multipath parameters inside each OFDM block. Considering the fact that doubly-selective channels are restricted to low-dimensional subspaces, several publications propose to use basis expansion models for further reducing the channel dimensions and consequently the required pilot overhead specifically for fast time-variant channels. Reference [5] proposes a reduced rank channel estimator for each sub-carrier using the discrete prolate spheroidal (DPS) sequences. While [5] uses the time domain correlation for each sub-carrier, [6] and [7] propose low-dimensional channel estimators based on the frequency domain correlation between sub-carriers via singular value decomposition (SVD) of the channel covariance matrix. Further improvement can be obtained through exploiting time and frequency correlation simultaneously. Papers [8] and [9] use the time and frequency correlation and adopt the multi-dimensional DPS sequences in [5] to remove the requirement of the known covariance matrix. In [8] successive Slepian subspace projection of the channel is used in time and frequency and in [9] the eigenvectors of the channel covariance matrix are approximated by a two-dimensional subspace model spanned by generalized-DPS (GDPS) sequences. In both papers, the channel estimation on different antennas are obtained one by one considering each antenna pair as a SISO-OFDM channel.

The 2D time-frequency DPS/GDPS sequences can be generalized to higher dimensions for exploiting the additional spatial correlation between the multi-antenna elements which is a common feature of most HSR scenarios that have a LOS component and limited number of scatterers due to the base station (BS) antenna heights and the distance of the BSs from the railway [1]. In [10], the projection of the known MIMO-OFDM channel coefficients onto 4D DPS sequences is used for low complexity implementation of a geometry-based channel model on a hardware channel simulator. For MIMO-OFDM channel estimation, However, to our best knowledge, none of the previous work has considered the extra spatial domain correlation together with the time and frequency correlation for obtaining a more accurate channel estimation with a lower pilot overhead. In this paper a reduced rank linear minimum mean square error (LMMSE) channel estimator is proposed based on a 4D basis expansion channel model which uses GDPS sequences for exploiting the time, frequency and spatial correlation at the transmitter and receiver antenna arrays of a time-variant frequency-selective MIMO-OFDM HSR channel. We validate the proposed time-variant channel estimator using a regular shape geometry-based stochastic model (RS-GBSM) for the propagation channel. The paper is organized as follows. The system model and RS-GBSM channel model are described in Sections 2 and 3, respectively. Section 4 presents a 4D GDPS channel model. Section 5 provides the corresponding reduced rank channel estimator. Simulation results and conclusion are provided in Sections 6 and 7, respectively.

Notation: We denote a scalar by a, a column vector by $\boldsymbol{a}$ with its i th element $\boldsymbol{a}[i]$ and a matrix by $\mathbf{A}$ with its i th row $\mathbf{A}[i,:]$. The inverse, transpose and Hermitian transpose of a matrix $\mathbf{A}$ is denoted by $\mathbf{A}^{-1}$, $\mathbf{A}^{T}$ and $\mathbf{A}^{H}$, respectively. $\mathbf{I}_n$ is an $n \times n$ identity matrix. We denote the set of complex numbers by $\mathbb{C}$, integers by $\mathbb{Z}$ and non-negative integers $\{0, 1, \ldots, k-1\}$ by $\mathbb{I}_k$. The smallest integer that is greater than or equal to a is denoted by $\lceil a \rceil$. The Kronecker product of $\boldsymbol{a}$ and $\boldsymbol{b}$ is $\boldsymbol{a} \otimes \boldsymbol{b}$.

2. System model

We consider a MIMO-OFDM system with each OFDM symbol containing N sub-carriers, and M_{T_x}-spatial data streams equipped with M_{T_x} and M_{R_x} transmit and receive antennas, respectively. The transmission at each transmit antenna is frame based with frame length of M OFDM symbols. The system bandwidth is B and the OFDM symbol duration is given by $T_s = (N+G)T_c$ with G being the cyclic prefix length and $T_c = 1/B$. The transmitted symbol at the mth OFDM symbol, qth sub-carrier and sth transmit antenna is defined as

$$d[m,q,s] = \begin{cases} b[m,q,s] & \text{if} \quad [m,q,s] \in \mathcal{S}_d \\ p[m,q,s] & \text{if} \quad [m,q,s] \in \mathcal{S}_p \\ 0 & \text{if} \quad [m,q,s] \notin \{\mathcal{S}_d \cup \mathcal{S}_p\} \end{cases} \tag{1}$$

where $b[m,q,s]$ and $p[m,q,s]$ is a QPSK modulated data and pilot symbol, respectively. $\mathcal{S}_d \in \mathbb{Z}^3$ indicates the set of integer data locations and $\mathcal{S}_p \in \mathbb{Z}^3$ indicates the set of integer pilot locations. The received signal $y[m,q,r]$ over the rth receive antenna is the superposition of M_{T_x} data symbols sent from M_{T_x} transmit antennas at time m and sub-carrier q. That is,

$$y[m,q,r] = \sum_{s=1}^{M_{T_x}} h[m,q,r,s]d[m,q,s] + z[m,q,r] \tag{2}$$

where $h[m,q,r,s]$ is the sampled channel frequency response and $z[m,q,r]$ is the complex white Gaussian noise component.

3. Geometry based stochastic model for Wideband MIMO HST channel

For modelling the channel, we use the multi-tap RS-GBSM which is proposed recently for non-stationary wideband MIMO channels in high mobility railway communication [11]. In this model the scatterers are assumed to be distributed over N_T confocal ellipses (N_T taps) with the BS and the receiver antenna arrays located at the foci. There are N_i effective scatterers on the ith ellipse with time varying AODs and AOAs. More details can be found in [11]. The channel is composed of the LOS component and non-LOS (NLOS) part, that is, the contribution from the diffuse scatterers in the environment. We can describe the channel by the time-variant transfer function $h(t,f,y,x) = h_{NLOS}(t,f,y,x) + h_{LOS}(t,f,y,x)$ with t, f, y and x denoting the time, frequency, position of the receive antenna on the receive antenna array and position of transmit antenna on the transmit antenna array, respectively. Let $\Delta_f = 1/(NT_c)$ denote the width of a frequency bin and Δ_x and Δ_y denote the distance between adjacent antennas in the transmit and receive antenna arrays, respectively. The sampled NLOS channel transfer function which is the superposition of the contribution from $P = \sum_{i=1}^{N_T} N_i$ multipath components is given

by

$$h_{NLOS}(m,q,r,s) = h_{NLOS}(mT_s, \varphi(q)\Delta_f, k_r(r)\Delta_y, k_s(s)\Delta_x)$$
$$= \sum_{i=1}^{P} \eta_i(m) e^{-j2\pi D_0/\lambda} e^{-j2\pi\tau_i(m)\varphi(q)\Delta_f} e^{j2\pi\upsilon_{max} m\cos(\phi_R^i(m)-\gamma_R)}$$
$$\times\ e^{j2\pi k_r(r)\Delta_y\cos(\phi_R^i(m)-\beta_R)/\lambda} e^{j2\pi k_s(s)\Delta_x\cos(\phi_T^i(m)-\beta_T)/\lambda} \quad (3)$$

where $\eta_i(m)$ is the time variant amplitude of the i th path. D_0 is the initial distance between the transmitter and receiver antenna arrays. $\tau_i(m)$ is the travel time of waves corresponding to the i th scatterer and $\upsilon_{max} = f_D T_s$ is the maximum normalized Doppler frequency. γ_R is the train angle of motion and $\phi_T^i(m)$ and $\phi_R^i(m)$ are the AOD and AOA of the ith scatterer. β_T, β_R are the tilt angles of transmit and receive antenna array relative to major axis of the ellipses, respectively. $\varphi(q) = (q + 0.5N)\text{mod}(N) - 0.5N$, $k_s(s) = 0.5(M_{T_x} - 2s + 1)$ and $k_r(r) = 0.5(M_{R_x} - 2r + 1)$ map the carrier index $q \in \{0, \ldots, N-1\}$, the transmit antenna index $s \in \{1, \ldots, M_{T_x}\}$ and the receive antenna index $r \in \{1, \ldots, M_{R_x}\}$ into the discrete frequency, transmit antenna position and receive antenna position indices, respectively. Similarly for the LOS channel we have

$$h_{LOS}(m,q,r,s) = \eta_{los}(m) e^{j\phi} e^{-j2\pi D_0/\lambda} e^{-j2\pi\tau_{los}(m)\varphi(q)\Delta_f}$$
$$e^{j2\pi\upsilon_{max} m\cos(\phi_{los}^s(m)-\gamma_R)} e^{j2\pi k_r(r)\Delta_y\cos(\phi_{los}^s(m)-\beta_R)/\lambda}$$
$$\times\ e^{j2\pi k_s(s)\Delta_x\cos(\beta_T)/\lambda} \quad (4)$$

where η_{los} is the real amplitude of LOS component. $\phi \in [-\pi, \pi)$ and $\tau_{los}(m) = D_s(m)/c$ where $D_s(m)$ is the time-variant distance between the BS and the train and c is the speed of the light. $\phi_{los}^s(m)$ is the time-variant LOS AOA corresponding to the sth transmit antenna [12]. η_i and η_{los} depend on the scattering environments and the channel Rician K factor which is different for different propagation scenarios. More information will be provided in Section 6.

4. Generalized discrete prolate spheroidal channel model

For channel estimation we propose to represent the MIMO-OFDM HSR channel in time, frequency and spatial domain by a low dimensional subspace and develop a low complexity linear minimum mean square error estimator for this channel model. Generally, LMMSE estimator requires the knowledge of the second order statistics [13] which are either difficult or impossible to be estimated in rapidly changing HSR channels. In order to obtain a reduced-rank LMMSE, the eigenvectors of the covariance matrix are considered as the optimal basis for spanning a low dimensional subspace [6]. In this section we approximate the time-variant eigenvectors of the channel covariance matrix by a 4D subspace model spanned by GDPS sequences, which does not need the knowledge of the channel covariance matrix but only the ranges of the channel support in space, time and frequency domains.

4.1. GDPS sequences

DPS sequences were first introduced by Slepian in 1987 [14]. They make a set of orthogonal basis that can span the same subspace U which is spanned by a time-concentrated and band-limited flat fading process with a symmetric spectral support $W = [-\nu_{max}, \nu_{max}]$. Later in [15], GDPS sequences were introduced by generalizing the concept of time-concentrated and band-limited sequences from a symmetric band-limiting interval to the union of I disjoint intervals, i.e., $W = W_1 \cup W_2 \ldots \cup W_I$. The M GDPS sequences $\{U_{d_t}^t[m, W, M]\}_{d_t=0}^{M-1}$ with band limitation to W and time concentration to $\mathbb{I}_M$ are the solutions to

$$\sum_{\ell=0}^{M-1} C[\ell - m, W] U_{d_t}^t[\ell, W, M]$$
$$= \lambda_{d_t}^t(W, M) U_{d_t}^t[m, W, M] \quad (5)$$

where in [15], $C[k, W]$ is shown to be proportional to the covariance function of a process with constant spectrum over W. The eigenvalue $\lambda_{d_t}^t(W, M)$ represents the energy concentration of $U_{d_t}^t[m, W, M]$ within $\mathbb{I}_M$. The essential dimension of the subspace U is given by [15]

$$D'(W, M) = \lceil |W| M \rceil + 1. \quad (6)$$

4.2. 4D GDPS channel model

In this section, based on the channel's band limitation in different domains, a 4D basis expansion model is used for the MIMO-OFDM HSR channel, which is similar to the 4D channel model presented in [10] but with the DPS basis being replaced by the GDPS sequences for having a more general model not necessarily being symmetric over its support in each domain. The maximum bandwidth of $h[m, q, r, s]$ is restricted to

$$W_{max} = W_t \times W_f \times W_x \times W_y \quad (7)$$

where $W_t = [-\upsilon_{max}, \upsilon_{max}]$, $W_f = [0, \theta_{max}]$, $W_x = [\zeta_{min}, \zeta_{max}]$ and $W_y = [\xi_{min}, \xi_{max}]$ are the maximum support of the channel in time, frequency, transmitter spatial domain and receiver spatial domain, respectively. $\theta_{max} = \tau_{max}\Delta_f$ indicates the maximum normalized delay of the channel and $\zeta_{min}(\xi_{min})$ and $\zeta_{max}(\xi_{max})$ are given by

$$\zeta_{max}(\zeta_{min}) = \max(\min)\{\cos(\phi_T^i(m) - \beta_T)\}\frac{\Delta_x}{\lambda}$$
$$\xi_{max}(\xi_{min}) = \max(\min)\{\cos(\phi_R^i(m) - \beta_R)\}\frac{\Delta_y}{\lambda} \quad (8)$$

where the maximization (minimization) is among all scatterers and over the whole frame. Note that each support contains at most P disjoint intervals corresponding to P scatterers. The band-limitation property of a MIMO-OFDM HSR channel allows us to represent the channel of all antennas over a frame of M OFDM symbols by the following 4D subspace model

$$h[m,q,r,s] = \sum_{d_t=0}^{D_t-1}\sum_{d_f=0}^{D_f-1}\sum_{d_y=0}^{D_y-1}\sum_{d_x=0}^{D_x-1} U_{d_t}^t[m, W_t, M]$$
$$U_{d_f}^f\left[\varphi(q) + \frac{N}{2}, W_f, N\right] U_{d_y}^y\left[k_r(r) + \frac{M_{R_x}}{2}, W_y, M_{R_x}\right]$$
$$U_{d_x}^x\left[k_s(s) + \frac{M_{T_x}}{2}, W_x, M_{T_x}\right] \psi_{d_t,d_f,d_y,d_x} \quad (9)$$

where $\{U^t_{d_t}[m, W_t, M]\}_{d_t=0}^{D_t-1}$, $\{U^f_{d_f}[q, W_f, N]\}_{d_f=0}^{D_f-1}$, $\{U^y_{d_y}[r, W_y, M_{R_x}]\}_{d_y=0}^{D_y-1}$,$\{U^x_{d_x}[s, W_x, M_{T_x}]\}_{d_x=0}^{D_x-1}$ span the time, frequency, receiver spatial domain and transmitter spatial domain subspaces, respectively. ψ_{d_t,d_f,d_y,d_x} is the corresponding weighting coefficient of the GDPS basis. D_t, D_f, D_y, D_x are the essential dimension of the subspaces obtained from (6). For modern high-rate communication systems, $\upsilon_{max} \ll 1$ which implies $|W_t| \ll 1$ and consequently $D_t \ll M$. Similarly, the maximum excess delay is limited in communication systems leading to $|W_f| \ll 1$ and so $D_f \ll N$. Considering the non-isotropic scattering with limited AOD and AOA spread and the proper distance between the antennas in transmit and receive antenna arrays, we also have $D_x \ll M_{T_x}$ and $D_y \ll M_{R_x}$.

5. Channel estimation

5.1. Problem formulation

Considering the channel model presented in (9), we can reformulate (2) as

$$\begin{aligned} y[m,q,r] = &\sum_{s=1}^{M_{T_x}}\sum_{d_t=0}^{D_t-1}\sum_{d_f=0}^{D_f-1}\sum_{d_y=0}^{D_y-1}\sum_{d_x=0}^{D_x-1} U^t_{d_t}[m]U^f_{d_f}\left[\varphi(q)+\frac{N}{2}\right] \\ &\times U^y_{d_y}\left[k_r(r)+\frac{M_{R_x}}{2}\right]U^x_{d_x}\left[k_s(s)+\frac{M_{T_x}}{2}\right] \\ &\times \psi_{d_t,d_f,d_y,d_x} d[m,q,s] \\ &+ z[m,q,r] \end{aligned} \tag{10}$$

where for notation simplicity, hereafter, we omit the index set and bandwidth notations previously used in the definition of GDPS basis. Using (10), the channel estimation problem is now reduced to estimation of the basis coefficients. The number of coefficients required to be estimated $|\psi_{d_t,d_f,d_y,d_x}| = D_tD_fD_yD_x \ll MNM_{R_x}M_{T_x}$. To obtain ψ_{d_t,d_f,d_y,d_x}, we can rewrite (10) in a matrix–vector form. We collect all basis coefficients in the vector Ψ with the following order,

$$\begin{aligned} &\Psi[d_tD_fD_yD_x + d_fD_yD_x + d_yD_x + d_x + 1] \\ &\quad = \psi_{d_t,d_f,d_y,d_x}. \end{aligned} \tag{11}$$

Similarly we define vectors $\boldsymbol{y}$ and $\boldsymbol{z}$ containing the received data values $y[m,q,r]$ and corresponding noise values $z[m,q,r]$ from all antennas over the transmitted frame as

$$\begin{aligned} &\boldsymbol{y}[mNM_{R_x} + qM_{R_x} + r + 1] = y[m,q,r] \\ &\boldsymbol{z}[mNM_{R_x} + qM_{R_x} + r + 1] = z[m,q,r]. \end{aligned} \tag{12}$$

From (11) and (12) we can define the final input–output relationship as

$$\boldsymbol{y} = \mathbf{D}\Psi + \boldsymbol{z} \tag{13}$$

where $\mathbf{D}$ is an $MNM_{R_x} \times D_tD_fD_yD_x$ matrix whose rows are given by

$$\begin{aligned} &\mathbf{D}\left[mNM_{R_x} + qM_{R_x} + r, :\right] \\ &\quad = \underbrace{\boldsymbol{f}^t[m] \otimes \boldsymbol{f}^f[q] \otimes \boldsymbol{f}^y[r]}_{D_1[m,q,r]} \otimes \boldsymbol{f}^d[m,q] \end{aligned} \tag{14}$$

with

$$\begin{aligned} \boldsymbol{f}^t[m] &= \left[U^t_0[m], \ldots, U^t_{D_t-1}[m]\right] \\ \boldsymbol{f}^f[q] &= \left[U^f_0\left[\varphi(q)+\frac{N}{2}\right], \ldots, U^f_{D_f-1}\left[\varphi(q)+\frac{N}{2}\right]\right] \\ \boldsymbol{f}^y[r] &= \left[U^y_0\left[k_r(r)+\frac{M_{Rx}}{2}\right], \ldots, U^y_{D_y-1}\left[k_r(r)+\frac{M_{Rx}}{2}\right]\right] \\ \boldsymbol{f}^x[s] &= \left[U^x_0\left[k_s(s)+\frac{M_{Tx}}{2}\right], \ldots, U^x_{D_x-1}\left[k_s(s)+\frac{M_{Tx}}{2}\right]\right] \\ \boldsymbol{f}^d[m,q] &= \sum_{s=1}^{M_{Tx}} \boldsymbol{f}^x[s]\, d[m,q,s]. \end{aligned} \tag{15}$$

Note that in (14), D_1 only depends on the GDPS basis and $\boldsymbol{f}^d$ is the pilot (data) dependent part.

5.2. LMMSE estimation of basis expansion coefficients

The linear estimator for the basis coefficient vector in (13) is expressed as [16]

$$\hat{\Psi}_{LMMSE} = \mathbf{C}^H_{\boldsymbol{y}\Psi}\mathbf{C}^{-1}_{\boldsymbol{yy}}\boldsymbol{y} \tag{16}$$

where $\mathbf{C}_{\boldsymbol{ab}} = \underset{d}{\mathbb{E}}\underset{\Psi}{\mathbb{E}}\underset{z}{\mathbb{E}}\left\{\boldsymbol{ab}^H\right\}$.

Calculating the covariance matrices, (16) is simplified to

$$\hat{\Psi}_{LMMSE} = \left(\tilde{\mathbf{D}}^H\Delta^{-1}\tilde{\mathbf{D}} + \mathbf{C}^{-1}_{\Psi}\right)^{-1}\tilde{\mathbf{D}}^H\Delta^{-1}\boldsymbol{y} \tag{17}$$

where $\tilde{\mathbf{D}}$ is obtained from $\mathbf{D}$ by replacing $d[m,q,s]$ at $[m,q,s] \in \mathcal{S}_d$, by zero. This means that only pilot symbols are used for channel estimation. The matrix Δ is given by

$$\Delta = \Lambda + \sigma^2_z\mathbf{I}_{MNM_{Rx}}, \tag{18}$$

where σ^2_z is the noise variance and the block-diagonal matrix Λ is expressed as

$$\begin{aligned} \Lambda\left[i_{m,q,r_1}, i_{m,q,r_2}\right] = &\frac{1}{|W_t||W_f||W_y||W_x|}\sum_{d_t=0}^{D_t-1}\sum_{d_f=0}^{D_f-1}\sum_{d_y=0}^{D_y-1}\sum_{d_x=0}^{D_x-1} \\ &\times \left\{\lambda^t_{d_t}\lambda^f_{d_f}\lambda^y_{d_y}\lambda^x_{d_x}\left|U^t_{d_t}[m]\right|^2 U^y_{d_y}[k_r(r_1)+\frac{M_{R_x}}{2}]\right. \\ &\times U^y_{d_y}[k_r(r_2)+\frac{M_{R_x}}{2}]^* \\ &\times \left|U^f_{d_f}[\varphi(q)+\frac{N}{2}]\right|^2\sum_{s=1}^{M_{T_x}}\left|U^x_{d_x}[k_s(s)+\frac{M_{T_x}}{2}]\right|^2 \\ &\left.\times\left(1-\left|\tilde{d}[m,q,s]\right|^2\right)\right\} \end{aligned} \tag{19}$$

with $i_{m,q,r_i} = mNM_{R_x} + qM_{R_x} + r_i$ for $i = 1, 2$ and $r_1, r_2 \in \{1, \ldots, M_{R_x}\}$. Moreover, for the presented 4D GDPS channel model the covariance matrix $\mathbf{C}_{\Psi}$ is given by

$$\mathbf{C}_{\Psi} = \frac{1}{|W_t|\,|W_f|\,|W_y|\,|W_x|}diag\left(\lambda_t \otimes \lambda_f \otimes \lambda_y \otimes \lambda_x\right) \tag{20}$$

with

$$\lambda_k = \left[\lambda^k_0, \ldots, \lambda^k_{D_k-1}\right] \quad \text{for} \quad k \in \{t, f, y, x\} \tag{21}$$

Table 1
Channel parameters for the RS-GBSM described in Section 3 [11].

D_0	D_{min}	γ_R	β_T	β_R	N_T	N_i	v_R	Δ_x	Δ_y
100 m	30 m	22.5°	22.5°	22.5°	10	50	100 (m/s)	$\lambda/2$	$\lambda/2$

contains the eigenvalues defined in Section 4.1 for each of the GDPS basis. It is clear from (17)–(21) that there is no need for the known channel correlation matrix in the proposed channel estimator.

6. Simulation results

In this section, we present the simulation results to evaluate the proposed channel estimator. We consider $M = 14$, $N = 128$, $M_{T_x} = M_{R_x} = 4$, $f_c = 1.8$ GHz, $T_s = 8$ μs, $B = 1/T_c = 20$ MHz and the channel parameters listed in Table 1 or specified otherwise. The maximum normalized Doppler spread is controlled by the train velocity v_R as $|W_t| = 2\upsilon_{max} = 2v_R f_c T_s/c$ and considering the adjacent channel taps are at distance T_c from each other, the maximum normalized delay spread is $|W_f| = \theta_{max} = N_T/N$. The time varying AODs and AOAs of different scatterers are chosen from the von Mises distribution [11] controlling the angular spread and correspondingly the maximum support of the channel in spatial domain based on (8).

Viaducts and cuttings are the two most common HSR propagation environments which are special and different from those in commercial cellular communication [1]. The measurements in [17] show that the propagation environment of terrain cutting is worse than viaduct. So we consider the cutting scenario for our simulation. The complex path amplitude of the scatterers diffused on the surface of two slopes of the train cutting (see Fig. 2 in [18]) is modelled as

$$\eta_i(t) = G_{0,DI}^{1/2}.c_i.\left(\frac{d_{ref}}{d_{T\to i}(t)\times d_{i\to R}(t)}\right)^{n_{DI}/2} \tag{22}$$

where c_i is the zero mean complex Gaussian gain of the ith scatterer. $n_{DI} = 3$, $G_{0,DI} = 23$ dB are the path loss exponent and reference power and $d_{T\to i}$ and $d_{i\to R}$ are the scatterer distance to the BS and to the train, respectively. The Rician K factor in the cutting scenario follows the log-normal distribution with the mean 0.94 dB and standard deviation 4.18 dB [18].

Fig. 1 compares the performance of the proposed GDPS-based channel estimator in terms of the normalized mean square error (NMSE) with the conventional interpolation based LS and MMSE estimators which require to first obtain the channel estimation at pilot positions and then use a 2D interpolation in time and frequency to obtain the channel coefficients at the rest of the sub-carriers for each antenna pair. The 3D diamond pilot pattern presented in [3] is used for multiplexing the pilots into the transmitted data stream. The pilot overhead of diamond grid is adjustable based on the essential dimension of the GDPS basis in time, frequency and transmitter spatial domain which according to (6) are proportional to the bandwidth of the channel in each domain. The proposed channel estimator has better performance than the LS estimator. However, the MMSE channel estimator outperforms the proposed scheme

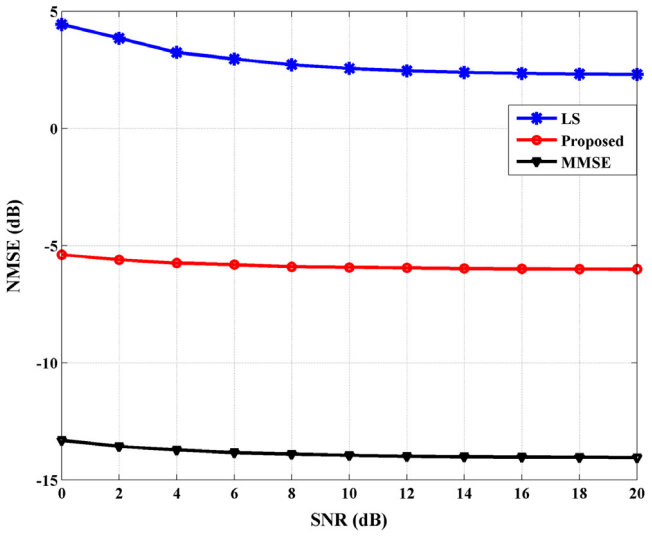

Fig. 1. Comparison of different estimators with the pilot overhead of 0.0135 for a 4 × 4 MIMO-OFDM system with $|W_t| = 0.0096$, $|W_f| = 0.0781$, AOA spread of 35.2° and AOD spread of 43.5°.

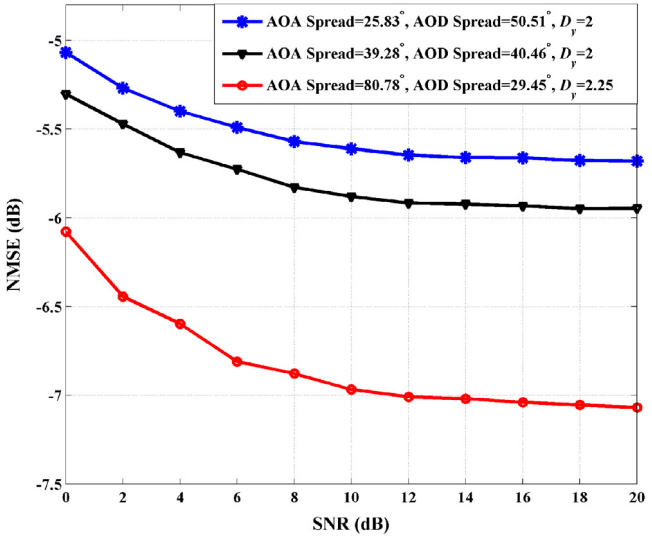

Fig. 2. Evaluation of the proposed channel estimator for different AOD/AOA spreads for a 4 × 4 MIMO-OFDM system with the pilot overhead of 0.0135, $|W_t| = 0.0096$ and $|W_f| = 0.0781$.

since the MMSE approach uses the full channel correlation information for both channel estimation at the pilot sub-carriers and interpolation at the data sub-carriers.

Fig. 2 shows the performance of the proposed channel estimator for different AOD and AOA spreads. For all cases it is assumed that $D_t = 2$, $D_f = 11$ and $D_x = 2$, leading to the same pilot overhead of 0.0135. Since the same number of basis are used for spanning the transmitter spatial domain, the

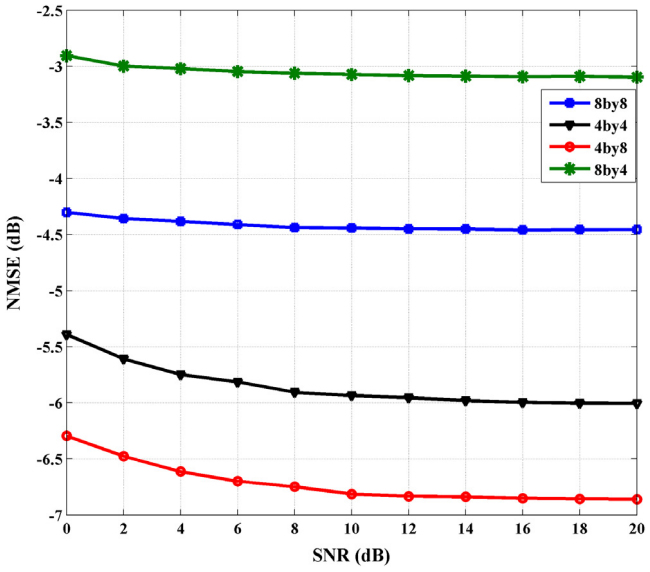

Fig. 3. Evaluation of the proposed channel estimator for different number of antennas with the pilot overhead of 0.0135, AOA spread of 35.2°, AOD spread of 43.5°, $|W_t| = 0.0096$ and $|W_f| = 0.0781$.

performance degrades for bigger AOD spreads. Moreover, for bigger AOA spreads more GDPS basis may be used for channel modelling which improves the estimation accuracy. The average D_y is indicated for each case. The effect of different antenna sizes is investigated in Fig. 3 for the same pilot overhead. Increasing the number of antennas will increase the number of basis used for channel modelling and can provide better channel approximation. However, for the transmitter array the increased number of antennas degrades the performance since the pilot overhead in the transmitter spatial domain is the same for all antenna sizes. For the receiver spatial domain, as the channel is sampled at all receive antennas we have enough samples for estimating the increased number of basis coefficients. So better performance is obtained for the bigger receiver antenna array sizes.

Fig. 4 represents the effect of different delay spreads on channel estimation accuracy. Each scenario has a distinct pilot overhead based on the distinct number of frequency domain basis. As the pilot overhead is adjusted to each scenario it is expected that the NMSE does not differ greatly for each case. Fig. 5 also indicates the performance of the proposed channel estimator for different Doppler spreads. It is obvious that for the same pilot overhead, the bigger the train velocity is, the worse it is the channel estimator performance.

The computational complexity of the proposed reduced rank LMMSE estimator (17) in terms of floating point operations, is determined by the dimension of $\tilde{\mathbf{D}} \in \mathbb{C}^{MNM_{Rx} \times D_t D_f D_y D_x}$ and is calculated as follows [19]

$$C_{GDPS} \approx 8MNM_{Rx}\left(D_t D_f D_y D_x\right)^2 + \frac{8}{3}\left(D_t D_f D_y D_x\right)^3, \quad (23)$$

while for a full rank LMMSE estimator in which the channel coefficients are estimated rather than the basis coefficients,

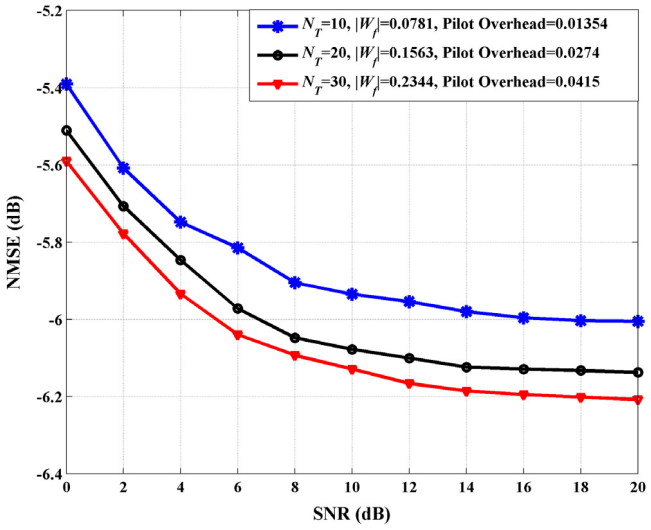

Fig. 4. Evaluation of the proposed channel estimator for different delay spreads with the AOA spread of 35.2°, AOD spread of 43.5° and $|W_t| = 0.0096$.

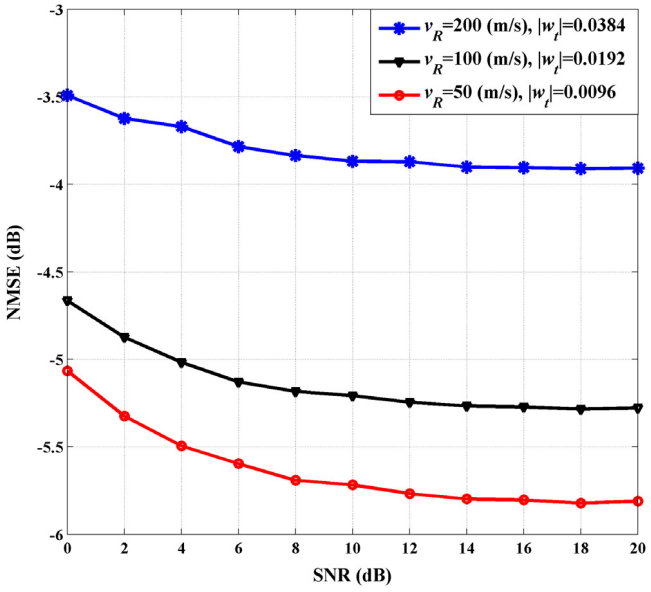

Fig. 5. Evaluation of the proposed channel estimator for different train velocities with $M = 28$, $T_s = 16$ μs, $B = 10$ MHz, AOA spread of 35.2°, AOD spread of 43.5° and $|W_f| = 0.0781$.

$\tilde{\mathbf{D}} \in \mathbb{C}^{MNM_{Rx} \times MNM_{Rx}M_{Tx}}$ and the computational complexity is

$$C_{full} \approx 8(MNM_{Rx})^3\left(M_{Tx}{}^2 + \frac{1}{3}M_{Tx}{}^3\right). \quad (24)$$

As an example, for the parameters presented in Table 1 with 8×8 MIMO size, $D_t = 2$, $D_f = 11$, $D_y = 3$ and $D_x = 3$, there is relative complexity reduction of $C_{full}/C_{GDPS} = 1.2246e + 06$.

7. Conclusion

Considering the time, frequency and spatial correlation of the MIMO-OFDM HSR channels, we have proposed a reduced rank LMMSE estimator based on a 4D GDPS channel

model. The low dimension of the basis resulted in the good performance of the GDPS based channel estimator compared to the conventional interpolation based LS and MMSE channel estimators for the same pilot overhead and with lower computational complexity. Simulation results, presented for the train cutting scenario and the non-stationary RS-GBSM channel model, have demonstrated the robust performance of the channel estimator for different antenna sizes and different Doppler, delay and angular spreads.

Conflict of interest

The authors declare that there is no conflict of interest in this paper.

References

[1] B. Ali, X. Cheng, T. Kurner, Z. Zhong, Challenges toward wireless communications for high speed railway, IEEE Trans. Intell. Transp. Syst. 15 (2014) 2143–2158.

[2] P. Hoeher, S. Kaiser, P. Robertson, Two-dimensional pilot symbol-aided channel estimation by wiener filtering, in: Proc. IEEE International Conference on Acoustics Speech and Signal Processing (ICASSP-97.), Munich, Germany, Apr. 1997, pp. 1845–1848.

[3] G. Auer, 3D MIMO-OFDM channel estimation, IEEE Trans. Commun. 60 (4) (2012) 972–985.

[4] B. Yang, K.B. Letaief, R.S. Cheng, Z. Cao, Channel estimation for OFDM transmission in multipath fading channels based on parametric channel modeling, IEEE Trans. Commun. 49 (3) (2001) 467–479.

[5] T. Zemen, C. Mecklenbrauker, Time-variant channel estimation using discrete prolate spheroidal sequences, IEEE Trans. Signal Process. 53 (2005) 3597–3607.

[6] O. Edfors, M. Sandell, J.J. van de Beek, S.K. Wilson, P.O. Brjesson, OFDM channel estimation by singular value decomposition, IEEE Trans. Commun. 46 (7) (1998) 931–939.

[7] J. Du, Y. Li, D-BLAST OFDM with channel estimation, EURASIP J. Appl. Signal Process. 5 (2004) 605–612.

[8] P.S. Rossi, R. Muller, Slepian-based two-dimensional estimation of time-frequency variant MIMO-OFDM channels, IEEE Signal Process. Lett. 15 (2008) 21–24.

[9] T. Zemen, L. Bernado, N. Czink, A.F. Molisch, Iterative time-variant channel estimation for 802.11p using generalized discrete prolate spheroidal sequences, IEEE Trans. Veh. Technol. 61 (2012) 1222–1233.

[10] F. Kaltenberger, T. Zemen, C.W. Uberhuber, low complexity geometry-based MIMO channel simulation, EURASIP J. Adv. Signal Process. 2007 (2007).

[11] A. Ghazal, C.X. Wang, B. Ali, D. Yuan, A nonstationary wideband MIMO channel model for high-mobility intelligent transportation systems, IEEE Trans. Intell. Transp. Syst. 16 (2) (2015) 885–897.

[12] 3rd Generation Partnership Project, Evolved universal terrestrial radio access (E-UTRA); base station (BS) radio transmission and reception, ETSI, Technical Specification 136 104 V11.8.2, 2014.

[13] F.A. Dietrich, W. Utschik, Pilot-assisted channel estimation based on second-order statistics, IEEE Trans. Signal Process. 53 (3) (2005) 1178–1193.

[14] D. Slepian, Prolate spheroidal wave functions, fourier analysis, and uncertaintyv: The discrete case, Bell Syst. Tech. J. 57 (5) (1978) 1371–1430.

[15] T. Zemen, C.F. Mecklenbruker, B.H. Fleury, F. Kaltenberger, Minimum-energy band-limited predictor with dynamic subspace selection for time-variant flat-fading channels, IEEE Trans. Signal Process. 55 (9) (2007) 4534–4548.

[16] T. Zemen, C.F. Mecklenbruker, J. Wehinger, R.R. Mller, Iterative joint time-variant channel estimation and multi-user detection for MCCDMA, IEEE Trans. Wireless Commun. 5 (6) (2006) 1469–1478.

[17] J. Lu, G. Zhu, C. Briso-Rodriguez, Fading characteristics in the railway terrain cuttings, in: Proc. IEEE Vehicular Technology Conference (VTC Spring 11), Yokohama, Japan, May 2011, pp. 1–5.

[18] B. Chen, Z. Zhong, Geometry-based stochastic modeling for MIMO channel in high-speed mobile scenario, Int. J. Antennas Propag. 2012 (2012) 1–6.

[19] C. Dumard, T. Zemen, Low-complexity MIMO multiuser receiver: A joint antenna detection scheme for time-varying channels, IEEE Trans. Signal Process. 56 (7) (2008) 2931–2940.